V. 88, N 5

JOURNAL OF APPLIED SPECTROSCOPY

## AVOIDING SELF-REVERSED D LINES IN LASER-INDUCED BREAKDOWN SPECTROSCOPY OF TRACE-LEVEL SODIUM IN SOIL

W. Hu <sup>1\*</sup>, L. E. Agelet <sup>3</sup>, X. K. Shen <sup>2</sup>, X. N. He <sup>2</sup>, H. Huang <sup>2</sup>, Y. F. Lu <sup>2</sup>

Pittsburgh, PA 15260, USA; e-mail: weh40@pitt.edu

Self-reversed sodium D lines in laser-induced plasmas generated from soil samples with a sodium trace concentration of 42.3 ppm was examined using laser-induced breakdown spectroscopy (LIBS). The inverse pulse-energy dependence as well as spatially resolved behaviors of self-reversal were investigated using a pulsed Nd:YAG laser (532 nm, 7 ns) and a spectrograph with an ICCD camera. As pulse energy increases, the degree of self-reversal first augments then rapidly diminishes. The mechanism behind this lies in the separation of emission and absorption centers in wavelength, coupled with the fact that the central and outer layers of the plasmas were heated up equally with higher pulse energies. This indicates the possibility of avoiding self-reversal in an active manner.

Keywords: laser-induced breakdown spectroscopy, Nd:YAG laser, spectrum.

## ПРЕДОТВРАЩЕНИЕ САМООБРАЩЕНИЯ *D*-ЛИНИЙ В ЛАЗЕРНО-ЭМИССИОННОЙ СПЕКТРОСКОПИИ СЛЕДОВЫХ КОЛИЧЕСТВ НАТРИЯ В ПОЧВЕ

W. Hu 1\*, L. E. Agelet 3, X. K. Shen 2, X. N. He 2, H. Huang 2, Y. F. Lu 2

УДК 543.423

Питтсбург, штат Пенсильвания 15260, США; e-mail: weh40@pitt.edu

Штат Линкольн, Небраска, 68588-0511, США

(Поступила 2 ноября 2020)

С помощью лазерно-эмиссионной спектроскопии (LIBS) исследованы самообратимые D-линии натрия в лазерно-индуцированной плазме, генерируемые из образцов почвы со следами концентрации натрия 42.3 ppm. Зависимость обратной энергии импульса от энергии, а также пространственно разрешенное поведение самообращения исследованы с использованием импульсного YAG:Nd-лазера (532 нм, 7 нс) и спектрографа с камерой ICCD. По мере увеличения энергии импульса степень самообращения увеличивается, затем быстро уменьшается. Механизм заключается в разделении центров излучения и поглощения по длине волны в сочетании с тем, что центральный и внешний слои плазмы нагреваются одинаково с более высокими импульсами энергии. Это указывает на возможность активного предотвращения самообращения.

**Ключевые слова:** лазерно-эмиссионная спектроскопия, YAG:Nd-лазер, спектр.

<sup>&</sup>lt;sup>1</sup> Department of Physics and Astronomy, University of Pittsburgh,

<sup>&</sup>lt;sup>2</sup> Department of Electrical and Computer Engineering, University of Nebraska-Lincoln, Lincoln, NE 68588-0511, USA

<sup>&</sup>lt;sup>3</sup> Department of Agricultural and Biosystems Engineering, Iowa State University, Ames, IA 50011, USA

<sup>&</sup>lt;sup>1</sup> Университет Питтсбурга,

<sup>&</sup>lt;sup>2</sup> Университет Небраски-Линкольна,

<sup>&</sup>lt;sup>3</sup> Государственный университет Айовы, Эймс, штат Айова 50011, США

Introduction. Pulsed laser ablation has been widely studied as a method of material removal from solid samples and deposition of thin films [1]. The general laser ablation technique was developed by the Smalley and Bondybey groups to produce gas-phase clusters of refractory metal or nonmetal elements [2, 3]. When an intense pulsed laser beam is focused on the surface of a solid target, a hot luminous plasma is generated whose intensity allows for qualitative or quantitative analysis of the interrogated sample. The major limitations of the so-called laser-induced breakdown spectroscopy (LIBS) for practical applications stem from self-absorption, line broadening, and strong matrix effects along with high intensity of the background continuum. Some limitations can be minimized or avoided using certain controlled ambient gas and employing temporally-resolved spectroscopic measurements or temporally-integrated and spatially resolved measurement techniques [4]. To attain more accurate concentration estimation of the elements contained in a target of interest, and to improve the LIBS sensitivity, some of these restricting factors have to be taken into account, such as self-absorption or self-reversal – a type of intense self-absorption that usually occurs in resonance spectral lines associated with the main constitutional or host elements in the target. Although the selfabsorption problem can be somehow bypassed by selecting specific transitions between high-lying energy levels of the element, they usually exhibit weak emission intensity due to less population in accordance with Boltzmann distribution. In the case of trace element detection, the strongest resonance lines (with their lower energy states being the ground states) are commonly employed. A naïve presumption is that self-absorption should not occur or at least be negligible for low density of trace element atoms. However, this is not always true, as the phenomenon is more prevalent than we expected and hard to avoided in certain cases of trace elements including alkali metals such as Na, which negatively affect the calibration accuracy. In spite of this, the self-reversal is otherwise an informative and facile measure of intrinsic plasma properties, in particular the distribution of population densities of upper- and lower-state atoms, the distribution of plasma electron density [5], and of species velocity [6].

We investigated the laser pulse energy (laser fluence) dependence of self-reversed Na D lines emitted by the ablation plasmas from the North American Proficiency Testing Program (NAPT) standard soil samples with trace amount of Na. The spatially integrated and spatially resolved spectra were obtained, respectively, for detailed study of the effects of main variables (pulse energy, axial position) on the spectral line self-reversal of the trace amount element considered and its correlation with the plasma properties.

**Results and discussion.** A schematic diagram of the experimental setup used for laser-induced plasmas in this study is shown in Fig. 1. A *Q*-switched Nd:YAG laser operating at 532 nm (Continuum, Powerlite Precision II 8010, pulse duration of 7 ns) was employed in the experiments, which was operated in the external trigger mode and synchronized by a digital delay generator (Stanford Research System DG535, 5-ps delay resolution). The repetition rate of the laser was 10 Hz. The Nd:YAG laser beam was focused onto a mechanically pressed pellet of the soil sample Quincy\_2007-101 with Na of 42.3 ppm, part of the reference standards from the Soil Science Society of America (SSSA), NAPT, with a normal incidence by a convex lens (focal length: 15 cm). To avoid overablation, the soil sample was mounted on a translation stage. The laser was focused to a spot size of around 1 mm in diameter. The experiments were performed in an open air.

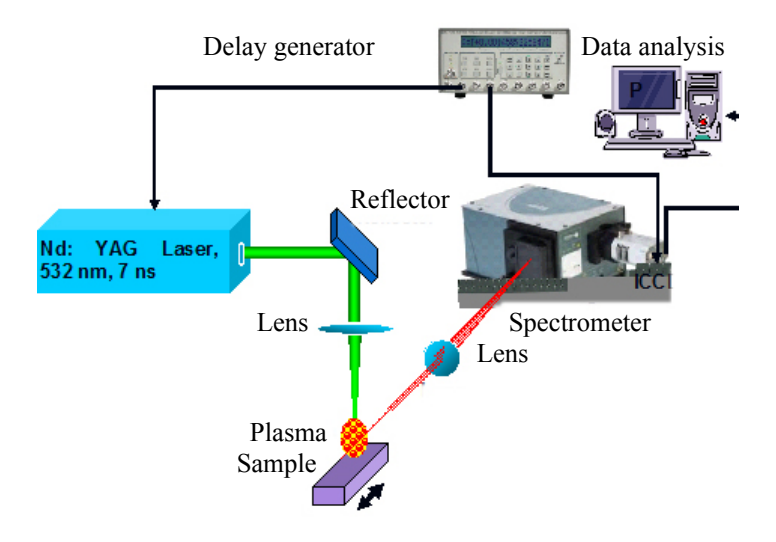


Fig. 1. Schematic diagram of the experimental setup.

The laser fluences for the Nd:YAG ranged from 0.5 to 38 J/cm². The size of the luminous plasmas was 1–7 mm in diameter dependent on the ablation energy used. The light emissions from the laser-induced plasma plumes were optically coupled to the entrance slit of a spectrometer (Andor Tech., Shamrock 303i) by a UV-grade quartz lens (focal length: 10 cm). The optical emissions at the center of the plasmas were analyzed by the spectrometer, which has three gratings with 150, 600, and 2400 lines/mm. The spectral resolution for the 2400-line grating is 0.1 nm. An intensified charge-coupled device with 512×512 pixels (ICCD: Andor Tech., iStar DH-712) was attached to the exit focal plane of the spectrometer to detect the spectrally resolved lines. The ICCD detector was operated in the gated mode, and the readout mode of the CCD was set as single or multi-track to obtain spatially integrated and resolved spectra. Data acquisition and analyses were performed on a personal computer. A total of 50, 100, or 1000 spectra, corresponding to 50, 100, or 1000 laser pulse events, was accumulated to produce one spectrum to increase the sensitivity of the system and to reduce statistical fluctuations.

Figure 2a shows a typical spectrum of self-reversed Na doublet lines emitted from the ablated plasmas from the pressed soil pellet of the NAPT standard sample with following its components (ppm): P - 95, K - 189, Ca - 1056, Mg - 251, Na - 42.3, S - 10.7, Al - 460, Zn - 5.88, Mn - 31, Fe - 287, Cu - 1, B - 0.5.

The gate width and delay time of the ICCD were set o 3 and 15  $\mu$ s, respectively. Figures 2b,c show the pulse energy (or fluence) dependence of the self-reversal phenomenon in the Na D lines of the stronger peak at 589.0 nm, where the degree of self-reversal is simply defined by the ratio  $r_{\rm sr} = (I_{\rm peak} - I_{\rm valley})/I_{\rm peak}$ , which is in our case chosen as an effective index to characterize the phenomenon qualitatively. As the pulse energy of the Nd:YAG laser increased from 5 mJ, the maximal intensity  $I_{\rm peak}$  increased accordingly, while the degree of self-reversal first rose rapidly from an initial value of 0.12 to a peak value of 0.33 at 17 mJ of pulse

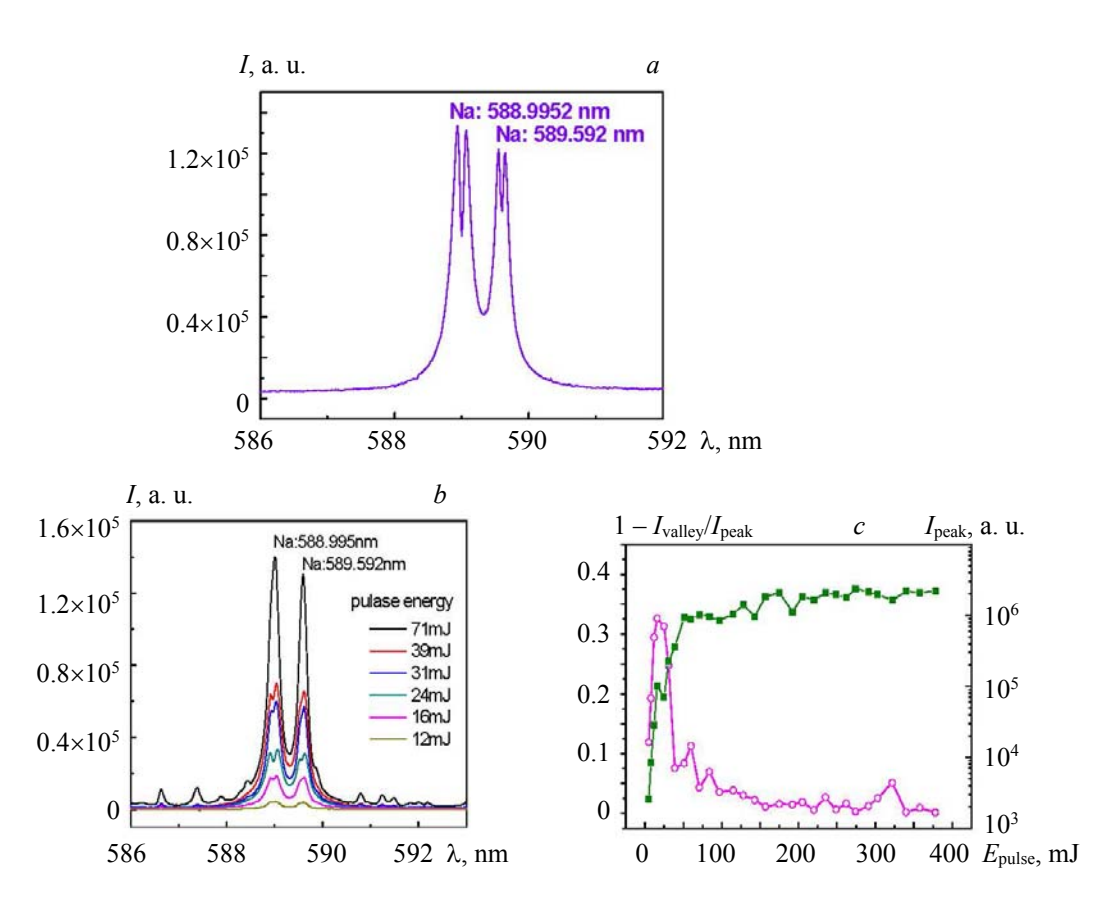


Fig. 2. a) A typical self-reversed Na spectral line collected from the ablation plasmas of the soil target 2007-101, integrated from 3–15  $\mu$ s after the laser pulse, with the slit aimed at the plasma center, accumulated over 1000 laser pulses. b, c) Pulse energy dependence of self-reversal phenomenon of the Na D lines for the stronger 589.0 nm peak, the diameter of laser focus is ~1 mm, the degree of self-reversal is defined as  $(I_{\text{peak}}-I_{\text{valley}})/I_{\text{peak}}$  ( $\circ$ ), along with  $I_{\text{peak}}$  ( $\bullet$ ).

energy, then dropped sharply to approach zero after 70–100 mJ of pulse energy. As is known, the selfreversal is a relatively intense self-absorption and is determined by the optical thickness of the lower energy state (the ground state in this case) associated with the relevant spectral line transition and the temperature difference between the outside layers and the central part of the plasmas. Here the temperature determines the relative population between the upper and lower states of the local Na atoms for the spectral transition concerned. Alternatively, it can also be accounted for by the difference in the so-called characteristic distribution length of the respective energy states [5]. Although the Na concentration is as low as 42.3 ppm, the Na atoms in the ablated plasmas are already sufficiently dense to generate an optically thick condition due to the low melting point of Na (370.9 K). When the laser pulse energy increased from 5 to ~16 mJ, the cloud of Na atoms produced became denser, which made it available for the cooler outer plasma (containing more ground-state Na atoms) to absorb light at the same wavelength emitted from the plasma core (containing more excited-state Na atoms). However, as the pulse energy continued to increase, the entire axially symmetric plasma plume was homogeneously heated up; hence the difference between the outer and inner temperatures became smaller [7]. Therefore, the outer plasma layer became transparent to the emission from the plasma core, leading to disappearance of the self-reversed valleys over the emission peaks. In addition, it can be seen that the self-reversal valleys are asymmetric, which originates from the mismatch of emission and absorption centers, to be elaborated later.

The Na concentration in the standard soil sample is at a trace level. Other reported elements need much higher concentrations in targets to produce the same self-reversal phenomenon for the resonance lines. In any quantitative analyses, self-absorption must be considered even if the concentration is at a trace level as long as resonance lines are involved, otherwise systematic error and inaccuracy is inevitable.

Spatially resolved spectra of Na D lines were obtained for detailed investigation of the self-reversal characteristics in the laser induced plasmas. The upper part of Fig. 3a shows a typical slit image taken immediately after a laser pulse with a fluence of 3.5 J/cm<sup>2</sup> using a slit width of 2500 μm. The central hot region indicates the plasma body, where a slit width of 50 µm aimed at the plasma center was used to obtain the spectra. The lower part presents the diffractogram of the narrow slit for which 10 tracks were employed to obtain a series of spatially resolved spectra, whose spectra are shown in Fig. 3b. From the spatially resolved spectra, one can clearly observe the self-reversed valleys (dips) on the top parts of the two Na D peaks at 589 and 589.6 nm. Figure 4 shows the corresponding peak maxima  $I_{\text{peak}}$ , indexes of self-reversal  $1 - I_{\text{valley}}/I_{\text{peak}}$ , and positions of the valley bottoms corresponding to the stronger one (589 nm, with twofold degeneracy than 589.6 nm and more prone to be self-reversed) of the doublet lines as functions of the axial position in the z direction from the sample surface. It can be seen from the curve of the peak intensity in the Fig. 4a that the plasma extends about 3-4 mm above the surface of the sample under a laser fluence of 3.5 J/cm<sup>2</sup>, where the maximum position for peak intensities is ~1.8 mm, lagging behind the position of the maximum selfreversal at ~2.7 mm. This phenomenon suggests a discrepancy between the spatial distribution of the emission intensity and that of the radial temperature gradient of plasma. The maximum self-reversal suggests that the temperature gradient along the cord of sight maximizes at ~2.7 mm above the sample surface. The selfabsorption consumes the radiant emission at the same wavelength, consistent with the spatial separation of the positions for the maximum values of emission intensity and self-absorption. The characteristics of the plasma depend on the evolution of its inner and outer structure, determined by the interaction of the initially formed plasma plume with the trailing part of the laser pulse (plasma screening), the confinement of the plasma by the surrounding air, as well as the deformation effect of the reflected shock wave generated during the plasma formation by the target surface. In the Fig. 4b, it can be seen that the wavelength position of the valley bottom varies along the axial position in the z direction and maximizes close to the sample surface. The red shift is ascribed to the Stark effect of electrons. Neglecting the ion broadening and the slight dependence on temperature, the full width at half maximum (FWHM)  $\Delta \lambda_{width}(x)$  and spectral shift  $\Delta \lambda_{shift}(x)$  are expressed as

$$\Delta \lambda_{\text{width}}(x) = w n_e(x), \tag{1}$$

$$\Delta \lambda_{\text{shift}}(x) = dn_e(x), \tag{2}$$

which w and d are the "Griem parameters" of the investigated transition [8], proportional to the local electron density that reaches its maximum near the surface and rises slightly at the forefront of the plasma, which is assmed to be simultaneously influenced by the confinement of the ambient air and the reflective shock wave that compresses the plasma to a higher density. Moreover, the minimal local electron density that corresponds to the minimum red shift occurs approximately at the same location of  $\sim 2-3$  mm above the surface

where the maximal self-reversal occurs. This can be explained by the fact that the distribution of the upper state atoms is closely connected to the electron density distribution, according to the role played by electron collision in the process of atom excitation [5]. The more electrons near the surface, the more uniform the plasma temperature. Vice versa, the lower the electron density away from the surface, the higher the population density of the ground-state atoms as opposed to the inner region, leading to a higher temperature gradient and higher degree of self-reversal. In Fig. 3b, the wavelength positions of the two maxima of the straddled self-reversed line of 589 nm, the blue end  $P_b$ , the red end  $P_r$ , as well as that of the valley bottom  $P_v$ , are indicated in the spectra. It can be observed from their trend of variation along the axial position (z direction) that the separation between the two maxima  $P_b$  and  $P_r$  tends to increase as the location rises, due to the increase in the degree of self-reversal. Moreover, the red shifts of these two maxima also increase towards the sample surface and maximize just above the surface, along with the valley bottom. The latter fact reveals that at this relatively low fluence the local electron density in the core region where the light emits varies in the same degree as that in the peripheral region where the absorption occurs.

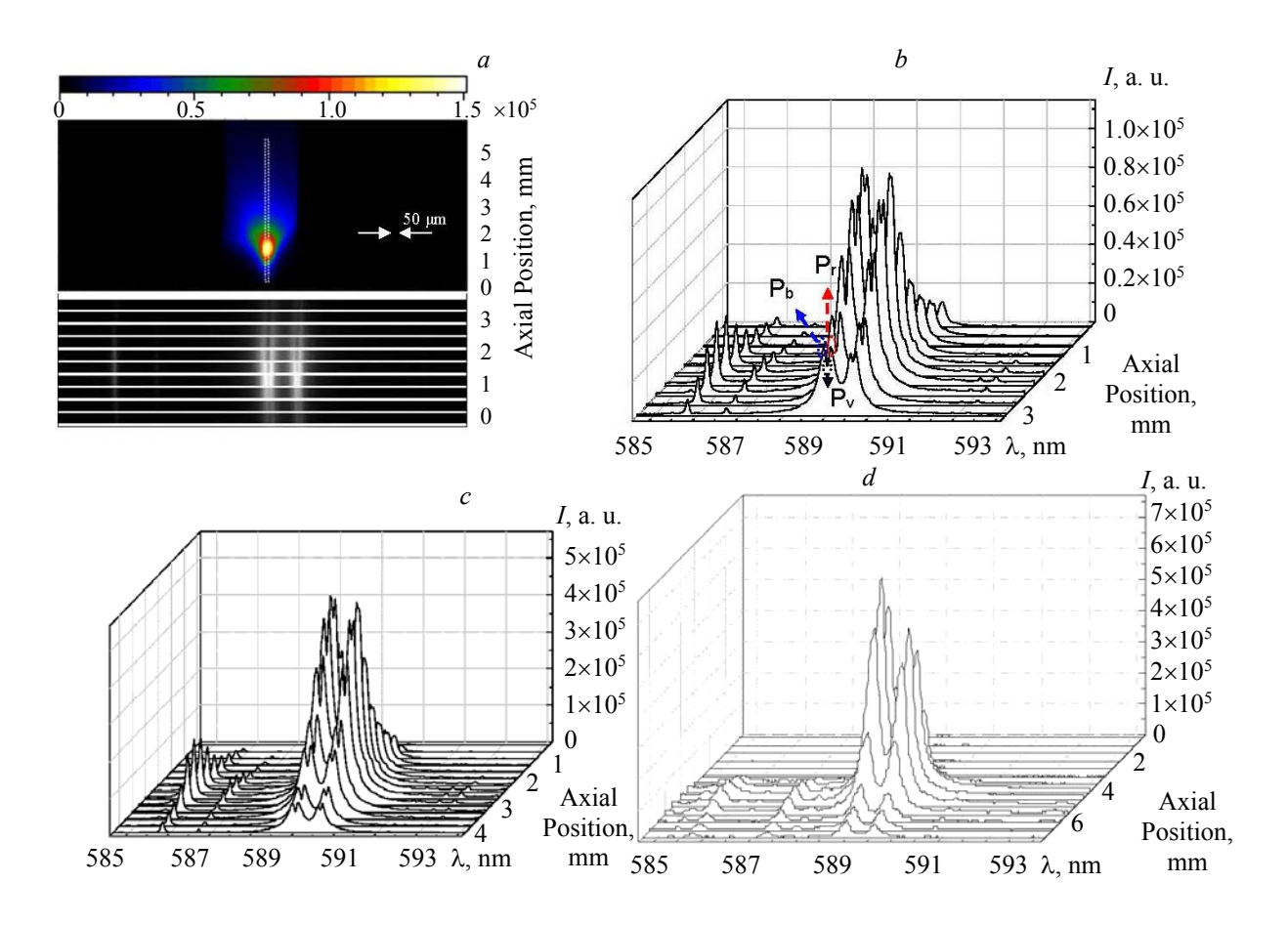


Fig. 3. a) A typical slit image taken immediately after laser pulse with a laser fluence of 3.5 J/cm<sup>2</sup> and a slit width of 2500 μm and diffractogram of the narrow slit for which 10–12 tracks were employed to attain a series of spatially-resolved spectra. The corresponding spatially-resolved spectra with a fluence of 3.5 (b), 5.4 (c), and 17 J/cm<sup>2</sup> (d).

The spatially resolved spectra with a higher laser fluence of 5.4 J/cm² are shown in Fig. 3c, for which 12 tracks were adopted to cover a bigger plasma plume. In this case, the location of maximum intensity of the 589.0 nm line rises from ~1.8 to ~2.1 mm above the surface, owing to plasma expansion. Moreover, the maximum red shift of the valley bottom observed near the sample surface increases to 0.12 nm compared to 0.09 nm with a lower fluence of 3.5 J/cm², consistent with a corresponding increase in electron density near the surface. Meanwhile, self-reversal near the sample surface almost disappears. A closer look shows, however, that this is not simply because of the homogeneous heating up of the plasma with an elevated fluence

level. While the red shift of emission light increases towards the sample surface and maximize nearby it, that of the valley bottom tends to be even larger, as illustrated in Fig. 5. This suggests that the atoms in the ground state have undergone a larger Stark effect than those in the excited state, possibly arising out of a locally intensified layer-structured electron density distribution (incidentally, following that of the plasmas density) near the sample surface, as a consequence of the stronger laser irradiation with a fluence of 5.4 J/cm<sup>2</sup>.

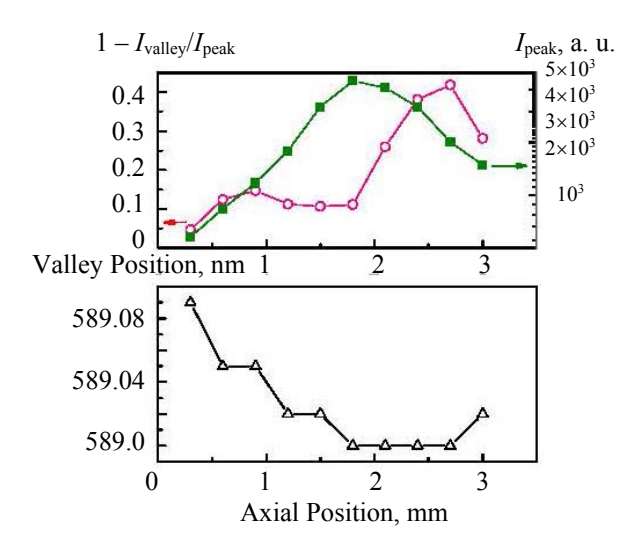


Fig. 4. a) Peak maxima  $I_{\text{peak}}$  ( $\blacksquare$ ) and indexes of self-reversal  $1 - I_{\text{valley}}/I_{\text{peak}}$  ( $\circ$ ). b) Positions of the valley bottoms for the 589 nm line as functions of the axial position, with a fluence of 3.5 J/cm<sup>2</sup>.

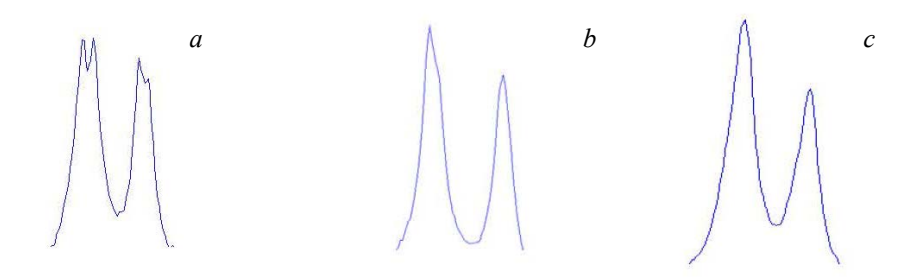


Fig. 5. Spatially-resolved spectra at  $\sim$ 0.3 mm above the sample surface with a fluence of 3.5 (a), 5.4 (b), and 17 J/cm<sup>2</sup> (c).

As the laser fluence increases up to  $17 \text{ J/cm}^2$ , no more apparent self-reversal could be observed in the same time scale of  $3-15 \mu s$ , as shown in Fig. 3d and Fig. 5c. Following the trend of the evolution as mentioned before, the disappearance of the self-reversal phenomenon thus originates from (i) the formation of a higher electron density in the periphery than in the core area, causing the difference between the wavelength centers of the line profiles corresponding to emission and absorption to become so large that they cannot overlap with each other, and (ii) the suppressed absorption in the periphery due to the homogeneous heating up of the plasma at higher fluences.

**Conclusions.** We studied the laser pulse energy (fluence) dependence of self-reversed Na D lines emitted by ablation plasmas from a NAPT standard soil sample at a trace Na concentration of 42.3 ppm. As pulse energy (fluence) increased, the degree of self-reversal first increased, then dropped rapidly to approach zero, in the meantime varying along the axial position above the sample surface. The mechanisms behind these phenomena are primarily due to the mismatch of wavelength centers of emission and absorption profiles by disparate Stark shifts and the uniform heating of the axially symmetric plasma plumes. This observation opens the possibility of actively avoiding self-reversal in LIBS.

This research was financially supported by the U.S. Office of Naval Research (ONR) through the Multidisciplinary University Research Initiative (MURI) program.

## REFERENCES

- 1. M. N. R. Ashfold et al., Chem. Soc. Rev., 33, 23 (2004).
- 2. T. G. Dietz et al., J. Chem. Phys., 74, No. 11, 6511 (1981).
- 3. J. L. Gole et al., J. Phys. Chem., 86, No. 14, 2560 (1982).
- 4. J. P. Singh, S. N. Thakur, Laser-induced Breakdown Spectroscopy, Elsevier Science (2007).
- 5. T. Sakka, T. Nakajima et al., J. Appl. Phys., 92, No. 5, 2296 (2002).
- 6. V. I. Mazhukin, V. V. Nossov et al., J. Phys. D: Appl. Phys., 37, 185 (2004).
- 7. M. Kuzuya, H. Aranami, Spectrochim. Acta B, 55, 1423 (2000).
- 8. H. R. Griem, *Plasma Spectroscopy*, McGraw-Hill, New York (1964).